BRAIN
A JOURNAL OF NEUROLOGY

Cohesin complex-associated holoprosencephaly

Paul Kruszka,[1] Seth I. Berger,[1,*] Valentina Casa,[2] Mike R. Dekker,[2] Jenna Gaesser,[3]
Karin Weiss,[1,‡] Ariel F. Martinez,[1] David R. Murdock,[1,♯] Raymond J. Louie,[4]
Eloise J. Prijoles,[4] Angie W. Lichty,[4] Oebele F. Brouwer,[5] Evelien Zonneveld-Huijssoon,[6]
Mark J. Stephan,[7] Jacob Hogue,[8] Ping Hu,[1] Momoko Tanima-Nagai,[1] Joshua L. Everson,[9,10]
Chitra Prasad,[11] Anna Cereda,[12] Maria Iascone,[13] Allison Schreiber,[14] Vickie Zurcher,[14]
Nicole Corsten-Janssen,[6] Luis Escobar,[15] Nancy J. Clegg,[16] Mauricio R. Delgado,[16,17]
Omkar Hajirnis,[18] Meena Balasubramanian,[19,20] Hülya Kayserili,[21] Matthew Deardorff,[22,23]
Raymond A. Poot,[2] Kerstin S. Wendt,[2] Robert J. Lipinski[9,10] and Maximilian Muenke[1]

Marked by incomplete division of the embryonic forebrain, holoprosencephaly is one of the most common human developmental disorders. Despite decades of phenotype-driven research, 80–90% of aneuploidy-negative holoprosencephaly individuals with a probable genetic aetiology do not have a genetic diagnosis. Here we report holoprosencephaly associated with variants in the two X-linked cohesin complex genes, *STAG2* and *SMC1A*, with loss-of-function variants in 10 individuals and a missense variant in one. Additionally, we report four individuals with variants in the cohesin complex genes that are not X-linked, *SMC3* and *RAD21*. Using whole mount *in situ* hybridization, we show that *STAG2* and *SMC1A* are expressed in the prosencephalic neural folds during primary neurulation in the mouse, consistent with forebrain morphogenesis and holoprosencephaly pathogenesis. Finally, we found that shRNA knockdown of *STAG2* and *SMC1A* causes aberrant expression of HPE-associated genes *ZIC2*, *GLI2*, *SMAD3* and *FGFR1* in human neural stem cells. These findings show the cohesin complex as an important regulator of median forebrain development and X-linked inheritance patterns in holoprosencephaly.

1 Medical Genetics Branch, National Human Genome Research Institute, National Institutes of Health, Bethesda, MD, USA
2 Department of Cell Biology, Erasmus MC, Rotterdam, The Netherlands
3 Department of Pediatrics, Division of Neurology, University of Pittsburgh, Pittsburgh, PA, USA
4 Greenwood Genetic Center, JC Self Research Institute of Human Genetics, Greenwood, SC, USA
5 Department of Neurology, University of Groningen, University Medical Center Groningen, Groningen, The Netherlands
6 Department of Genetics, University of Groningen, University Medical Center Groningen, Groningen, The Netherlands
7 Department of Pediatrics, University of Washington, Seattle, WA, USA
8 Division of Clinical Genetics, Department of Pediatrics, Madigan Army Hospital, Tacoma, WA, USA
9 Department of Comparative Biosciences, School of Veterinary Medicine, University of Wisconsin-Madison, Madison, WI, USA
10 Molecular and Environmental Toxicology Center, School of Medicine and Public Health, University of Wisconsin-Madison, Madison, WI, USA
11 Children's Health Research Institute, London, N6A 5W9, ON, Canada
12 Department of Pediatrics, ASST Papa Giovanni XXIII, Bergamo, Italy
13 Laboratorio di Genetica Medica, ASST Papa Giovanni XXIII, Bergamo, Italy
14 Genomic Medicine Institute, Cleveland Clinic, Cleveland, OH, USA
15 Peyton Manning Children's Hospital at St. Vincent, Medical Genetics and Neurodevelopment Center, Indianapolis, IN, USA
16 Texas Scottish Rite Hospital for Children, Dallas, TX, USA
17 Department of Neurology and Neurotherapeutics UT Southwestern Medical Center Dallas, TX, USA
18 Pediatric Neurology, Synapses Child Neurology and Development Centre, Thane, Maharashtra, India
19 Sheffield Clinical Genetics Service, Sheffield Children's, NHS Foundation Trust, Sheffield, UK
20 Academic Unit of Child Health, University of Sheffield, Sheffield, UK

21　Medical Genetics, Medical Faculty, Koç University, Istanbul, Turkey
22　The Division of Genetics, The Children's Hospital of Philadelphia, Philadelphia, PA, USA
23　The Department of Pediatrics, The Perelman School of Medicine, The University of Pennsylvania, Philadelphia, PA, USA

*Present address: Center for Genetic Medicine Research, Children National Health System, Washington, DC, USA
‡Present address: Genetics Institute, Rambam Health Care Campus, Haifa, Israel
♯Present address: Baylor College of Medicine, Houston, TX, USA

Correspondence to: Maximilian Muenke, MD
35 Convent Drive, Building 35 Room 1B203, Bethesda, MD 20892, USA
E-mail: mamuenke@mail.nih.gov

Correspondence may also be addressed to: Paul Kruszka, MD
35 Convent Drive, Building 35 Room 1B207, Bethesda, MD 20892, USA
E-mail: paul.kruszka@nih.gov

Introduction

Holoprosencephaly (HPE) is defined by incomplete division of the embryonic forebrain. While occurring in approximately 1 in 10 000 live births, HPE is estimated to occur in 1 in 250 embryos, making it one of the most common human developmental abnormalities (Matsunaga and Shiota, 1977). The most common cause is trisomy 13, which accounts for ∼50% of all cases (Kruszka and Muenke, 2018). Over the past two decades, four principal genes have been associated with HPE: *SHH* at 7q36.3, *ZIC2* at 13q32.3, *SIX3* at 2p21, and *TGIF1* at 18p11.31. These four genes have been the mainstay for genetic testing in individuals with HPE and normal karyotypes (Pineda-Alvarez *et al.*, 2010; Kruszka *et al.*, 2018). At least 10 other genetic loci have been associated with HPE, but at a lower prevalence (Kruszka *et al.*, 2018). *SHH*, *SIX3*, *ZIC2* and *TGIF1* account for only a fraction of the genetic aetiology in individuals with normal karyotypes. In a recent next generation sequencing study of 257 individuals with HPE, deleterious variants in *SHH* were most common in 5.8% of the HPE cohort, *ZIC2* at 4.7%, *SIX3* at 2.7% and no deleterious variants in *TGIF1* (Dubourg *et al.*, 2016); collectively, these four genes accounted for 13.2% of the aetiology in these individuals. With the introduction of whole exome sequencing (WES), driver mutations in new genes including *FGFR1* and *CNOT1* are being found (Simonis *et al.*, 2013; De Franco *et al.*, 2019; Kruszka *et al.*, 2019). To expand the genetic aetiology of HPE and uncover novel regulators of forebrain development, we have applied WES to 277 probands with HPE and both their parents (trios), if available.

We initially identified loss-of-function (LOF) variants in cohesin complex genes in 5 of 277 (1.8%) individuals in our holoprosencephaly cohort at the National Human Genome Research Institute (NHGRI). Through our holoprosencephaly network, DECIPHER (Firth *et al.*, 2009), and GeneMatcher (Sobreira *et al.*, 2015), we identified 10 other individuals with holoprosencephaly and variants in cohesin complex genes. Collectively, these 15 individuals with HPE have 13 LOF variants, one in-frame deletion, and one pathogenic missense variant distributed across the four cohesin complex genes *SMC1A* (MIM: 300040), *STAG2* (MIM: 300826), *SMC3* (MIM: 606062) and *RAD21* (MIM: 606462). The majority of cases (11/15) are females with variants in the X-linked genes *SMC1A* and *STAG2*. Cohesin is a highly conserved multiprotein complex with SMC1A, SMC3, RAD21 and STAG1/ STAG2 as its subunits in mammals (Brooker and Berkowitz, 2014). This complex forms a ring structure that is involved in sister chromatid cohesion during DNA replications. Additional roles of this complex include transcription regulation and DNA repair (Mehta *et al.*, 2013). Mutations in the cohesin complex and its regulators have been associated with four human genetic syndromes: Cornelia de Lange syndrome (CdLS) caused by variants in *NIPBL* (Krantz *et al.*, 2004), *SMC1A* (Musio *et al.*, 2006), *SMC3* (Deardorff *et al.*, 2007), *RAD21* (Deardorff *et al.*, 2012*b*), *BRD4* (Olley *et al.*, 2018), *HDAC8* (Deardorff *et al.*, 2012*a*); Roberts SC phocomelia syndrome caused by mutations in *ESCO2* (Gordillo *et al.*, 2008), CHOPS syndrome (Cognitive impairment and coarse facies, Heart defects, Obesity, Pulmonary involvement, and Short stature and skeletal dysplasia) associated with *AFF4* variants (Izumi *et al.*, 2015); and chronic atrial and intestinal dysrhythmia caused by mutations in *SGOL1* (Chetaille *et al.*, 2014). The cohesin complex genes that we associate with holoprosencephaly (*STAG2*, *SMC1A*, *SMC3* and *RAD21*) are intolerant of variation based on the Genome Aggregation Database (gnomAD) constraint metric of observed/expected loss of function (o/e) values (Lek *et al.*, 2016). Values <0.35 (o/e) are considered under selection against LOF (https://gnomad.broadinstitute.org) and the cohesin complex genes were well below this threshold: *STAG2* 0.02 [90% confidence interval (CI), 0.1–0.09], *SMC1A*

0.0 (90%CI, 0.0–0.06), *SMC3* 0.0 (90%CI, 0.0–0.04) and *RAD21* 0.1 (90%CI, 0.04–0.26).

Materials and methods

Subjects and clinical phenotyping

The individuals and families with HPE in this study were recruited from multiple international clinical genetics centres. Within the participating institutions, the phenotype was evaluated by clinical exam by the authors of this study and brain imaging (MRI or CT) or autopsy to confirm HPE. The study was approved by National Human Genome Research Institute Institutional Review Board (IRB) and the ethical committee of the patient's local institutions. The subjects' consents were obtained according to the Declaration of Helsinki.

DNA sequence analysis

Sanger sequencing

With the goal of new gene discovery, probands were pre-screened for four common genes known to cause HPE: *SHH* (MIM 600725) on 7q36, *ZIC2* (MIM 603073) on 13q32, *SIX3* (MIM 603714) on 2p21, and *TGIF1* (MIM 602630) on 18p11.3 using Sanger sequencing (Supplementary material). Novel variants found in this study by WES were also confirmed with Sanger sequencing.

Whole exome sequencing

WES was performed at the National Intramural Sequencing Center (NISC) on the individuals from the NHGRI HPE cohort (Supplementary material). The remaining individuals were sequenced at seven other academic and commercial laboratories (Supplementary Table 1). All WES results were verified by Sanger sequencing. Stringent variant filtering of the NHGRI cohort included: (i) *de novo* inheritance of variants in genes known to be intolerant of variation (Lek *et al.*, 2016); (ii) absence in the ExAC data base (Lek *et al.*, 2016); and (iii) combined annotation-dependent depletion (CADD) scores >20 (Kircher *et al.*, 2014).

Mouse embryo *in situ* hybridization

Genes that contribute to median forebrain morphogenesis and HPE pathogenesis are expressed in the prosencephalic neural folds that give rise to the forebrain during primary neurulation (Roessler *et al.*, 2018). We therefore examined expression of *Stag2* and *Smc1a* by *in situ* hybridization on mouse embryos at GD8.25 (Supplementary material), a stage representing early neurulation and within the critical period for HPE genesis (Heyne *et al.*, 2015a). *In situ* hybridization was conducted as previously described and analysis was limited to the prosencephalic regions of the neural fold from which the forebrain will develop (Everson *et al.*, 2017). This study was conducted in strict accordance with the recommendations in the 'Guide for the Care and Use of Laboratory Animals' of the National Institutes of Health. The protocol was approved by the University of Wisconsin-Madison School of Veterinary Medicine Institutional Animal Care and Use Committee (protocol number 13–081.0). CD-1 mice (*Mus musculus*)

were purchased from Charles River and C57BL/6J mice from The Jackson Laboratory. Timed pregnancies were established as described previously (Heyne *et al.*, 2015b). Embryos were dissected at gestational Day 8.25 and fixed overnight in 4% paraformaldehyde. *In situ* hybridization was carried out on whole C57BL/6J embryos or 50-μm sections cut from CD-1 embryos with a vibrating microtome in the transverse plane along the anterior-posterior axis. *In situ* hybridization was carried out as described previously (Everson *et al.*, 2017).

Gene expression studies in human neural stem cells

To test the hypothesis that variation in cohesin genes, specifically *STAG2* and *SMC1A*, perturb known forebrain developmental pathways, we measured selected gene expression associated with these pathways. First, knockdown of *STAG2* and *SMC1A* with shRNA was performed on H9-derived human neural stem cells (ThermoFisher/Invitrogen, #N7800–100) (Supplementary material and Supplementary Fig. 1). Known HPE pathways were analysed at the gene expression level with RT-qPCR of *SHH*, *SIX3*, *FGFR1*, *GLI2*, *ZIC2*, *GLI2*, *SMAD3* and *DISP1* genes.

Data availability

The raw data that support the findings of this manuscript are available upon request to the corresponding author.

Results

Patients: phenotype and genotype

We assembled 277 individuals with HPE in our NHGRI cohort (135 trios and 142 singletons); the cohort characteristics are shown in Supplementary Table 2. In the four classic HPE genes, pathogenic variants were found in 33 (11.9%) individuals: *ZIC2* was most common with 15 (5.4%) variants, followed by *SHH* nine (3.2%), *SIX3* eight (2.9%), and *TGIF1* one (0.4%). For these four genes, Supplementary Table 3 lists each variant, HPE subtype and inheritance pattern. In our HPE cohort of 277 individuals at NHGRI, four females had truncating variants (four nonsense and one splice site) in the cohesin complex genes *STAG2* and *SMC1A* on the X chromosome, and one proband had a nonsense variant in *RAD21* on chromosome 8. Another four LOF variants in *STAG2* in females, two LOF variants and one missense variant in *SMC1A* all in females, two LOF variants in *RAD21*, and an in-frame deletion in *SMC3* were found through our group's HPE network, DECIPHER (Firth *et al.*, 2009) and GeneMatcher (Sobreira *et al.*, 2015) (genotypes: Table 1; phenotypes: Tables 2–5).

STAG2

The phenotypes of four of six patients with *STAG2* pathogenic variants in the present study included the most severe forms of HPE: alobar HPE with cyclopia, alobar without

Table 1 Individuals with HPE and variants in cohesin complex genes

Patient ID	Gene	Variant	hg19/GRCh37 human reference genome	Inheritance	CADD score	Age	HPE type
1	STAG2	c.3034C>T p.(R1012*)	chrX-123217380-C-T	De novo	53	Newborn	Alobar
2	STAG2	c.205C>T p.(Arg69*)	chrX-123164892-C-T	De novo	27	2 years	Semi-lobar
3	STAG2	c.436C>T p.(R146*)	chrX-123176469-C-T	Singleton	38	32-week gestation	Alobar
4	STAG2	c.2533+1G>A	chrX-123205174-G-A	Maternal	34	Newborn/deceased	Semi-lobar
5	STAG2	c.2898_2899del p.(Glu968Serfs*15)	chrX-123215352–123215353	De novo	36	12 months	Microform
6	STAG2	c.775C>T p.(Arg259*)	chrX-123181311-C-T	De novo	25.1	9.5 years	Septo-optic dysplasia
7	SMC1A	c.3285+1G>C	chrX-53409426-C-G	De novo	39	15 months	MIHV
8	SMC1A	c.1495C>T p.(Arg499*)	chrX-53436043-G-A	Singleton	28.5	16.5 months	Microform
9	SMC1A	c.2683C>G (p. Arg895Gly)	chrX-53423417-G-C	De novo	35	6 years	Semi-lobar/lobar
10	SMC1A	c.2394delA; p.(Lys798Asnfs*31)	chrX-53430524	De novo	35	3 years	Semi-lobar
11	SMC1A	c.2834delG; p.(Gly945Alafs*19)	chrX-53423175	De novo	35	20 months	Semi-lobar
12	RAD21	c.1548delinsTC p.Glu518Argfs*19	chr8-117862929	Paternally inherited	35	7 years	MIHV
13	RAD21	c.589C>T p.(Gln197*)	chr8-117869605-G-A	Unknown	38	14 years	HPE
14	RAD21	c.1217_1224del p.(Lys406Argfs*4)	chr8-117864885	Unknown	35	2 years	Septo-optic dysplasia
15	SMC3	c.1138_1152del p.(Gly380_Gln384del)	chr10-112343987-GG…AG (15 bp)	De novo	21.9	Termination after 21 weeks	Semi-lobar

CADD = combined annotation-dependent depletion; MIHV = middle interhemispheric variant type holoprosencephaly.

cyclopia, and semilobar HPE (Patients 1–4; Tables 1 and 2). The other two patients with *STAG2* variants had milder forms of HPE (Patients 5–6; Table 1): Patient 5 had microform HPE, which is characterized by midline clefting, hypotelorism and depressed nasal bridge without brain anomalies (Fig. 1B), and Patient 6 is classified with septo-optic dysplasia type of HPE (Hahn *et al.*, 2010) based on ophthalmology exam showing optic nerve hypoplasia and MRI findings of a mildly dysmorphic neurohypophysis. In Table 2, we compare the genotypes and phenotypes of the six cases in the present study with six cases with LOF variants from the medical literature (Mullegama *et al.*, 2017; Aoi *et al.*, 2019; Yuan *et al.*, 2019). Overlapping clinical features of the six individuals in the present study and the six individuals in the medical literature include two of the six cases from the medical literature with HPE: Patient 1 from Aoi *et al.* (2019) has a structural brain malformation consistent with HPE, and Patient 3 from Yuan *et al.* (2019) has the microform HPE subtype. Additionally, three of the four cases in the medical literature have midline brain malformations including HPE as noted above, agenesis of the corpus callosum, and dysgenesis of the corpus callosum. Most of the present study and the cases in the medical literature have vertebral anomalies: six of seven that reported spine anomalies. Vertebral anomalies are not part of the clinical features associated with classic CdLS, but are commonly found in individuals with variants in *SMC3* and *RAD21* (Kline *et al.*, 2018). Also, seven of nine total had congenital heart disease. All LOF *STAG2* variants in the medical literature are *de novo*; interestingly, in the present study, Patient 4, (1/5) is inherited maternally which may be explained by skewed X-inactivation (not tested) or incomplete penetrance. Additionally, there is a LOF variant in the gnomAD database of presumptively healthy individuals (allele count 1/178 804), which raises the possibility of the rare case of incomplete penetrance (https://gnomad. broadinstitute.org accessed 1 May 2019). Collectively from the 12 cases in the present study and medical literature with LOF variants in *STAG2*, only one individual was male and he was reported to have HPE (Aoi *et al.*, 2019); the most likely conclusion is that LOF variants in *STAG2* are lethal or result in the most severe phenotype (HPE). Coincidentally, Mullegama *et al.* (2017) reported a patient with a *STAG2* with an identical variant as in Patient 2 (Fig. 1), c.205C>T; p.Arg69*. The patient in the Mullegama *et al.* (2017) report had dysgenesis of the splenium of the corpus callosum and the patient in this study had semilobar HPE, showing that *STAG2* LOF variants are responsible for a spectrum of midline brain anomalies.

SMC1A

The other five individuals with X-linked HPE were all females (Patients 7–11) (Table 3 and Fig. 1D–F) with four truncating variants and one with a missense variant in *SMC1A*, a cohesin complex gene known to be associated with CdLS (Deardorff *et al.*, 2007). Variants in *SMC1A* account for 4–6% of individuals with CdLS (Patients

Table 2 Phenotype details of individuals with LOF variants in STAG2

	Present study						Mullegama et al., 2017	Aoi et al., 2019		Yuan et al., 2019		
	Patient 1	Patient 2	Patient 3	Patient 4	Patient 5	Patient 6		Patient 1	Patient 2	Patient 1	Patient 2	Patient 3
Variant	c.3034C>T p.(R1012*)	c.205C>T p.(Arg69*)	c.436C>T p.(R146*)	c.2533+1G>A	c.2898_2899del p.(Glu968Serfs*15)	c.775C>T p.(Arg259*)	c.205C>T p.(Arg69*)	c.3097C>T p.(Arg1033*)	c.2229C>T p.(Trp743*)	c.418C>T p.Q140*	c.1605T>A p.C535*	c.1658_1660delinsT p.K533lfs*6
Inheritance	De novo	De novo	Singleton	Maternal	De novo	De novo	De novo	De novo	De novo	De novo	De novo	De novo
Sex	Female	Female	Female	Female	Female	Female	Female	Male	Female	Female	Female	Female
Age	Newborn	2 years	32-week gestation	Newborn/deceased	12 months	9.5 years	8 years	foetus	7 years	3.7 years	4.5 years	1.9 years
Brain MRI/HPE type	Alobar	Semi-lobar	Alobar[a]	Semi-lobar	Microform	Septo-optic dysplasia	Dysgenesis of the splenium of the corpus callosum	HPE (unspecified)	White matter hypoplasia	NR	NR	Microform; agenesis of corpus callosum; colpocephaly
Developmental delay	NA	Global	NA	NA	+	Intellectual disability; motor delay;	Speech	NR	Intellectual disability; developmental delay	Motor and speech delay	Intellectual disability; motor and speech delay	Intellectual disability; motor and speech delay
Craniofacial anomalies	Midline cleft lip/palate	Cleft palate; micrognathia	Cyclopia; absent nose, microsomia, hypognathia	–	NR	–	Submucous cleft palate	Cleft lip/palate	Cleft palate	–	Micrognathia	Single central incisor; micrognathia
Microcephaly	+	+	+	Severe	+	–	+	+	–	–	+	+
Ear anomalies and hearing	Low-set	–	Hypoplastic right ear	NR	NR	–	Bilateral microtia with hearing loss	NR	Hearing loss	Dysmorphic ears	Microtia, right; conductive hearing loss	Dysmorphic ears
Vertebral anomalies	Lumbar spina bifida	–	T7–T10 hemivertebrae	NR	NR	NR	Thoracic hemivertebrae and butterfly vertebrae	NR	Thoracic hemivertebrae	Vertebral clefts	NR	+
Congenital heart disease	NR	Patent foramen ovale and patent ductus arteriosus	Ventricular septal defect	Hypoplastic left heart; DORV	–	Ventricular septal defect	Ventricular septal defect	Hypoplastic left heart	–	Hypoplastic left heart	NR	NR
Growth delay	NR	+	NA	NA	+	–		NR	Short stature	–	+	+
Limb anomalies	-	–	NR	–	NR	Left hip dysplasia	Bilateral fifth finger clinodactyly	NR	NR	–	Fifth finger clinodactyly	–
Other	Gastroesophageal reflux and has a G-tube and Nissen fundoplication		Duodenal atresia			Bilateral optic nerve hypoplasia			Seizure disorder	Seizure disorder		Seizure disorder

DORV = double outlet right ventricle; NA = non-applicable; NR = not reported.
[a]Autopsy finding.

Figure 1 Patient images. (**A**) Patient 3 with alobar HPE and a c.436C > T p.(Arg146*) variant in *STAG2*; (**B**) Patient 5 with microform HPE and a c.2898_2899del p.(Glu968Serfs*15) in *STAG2*; (**C**) Patient 2 with semi-lobar HPE and a c.205C > T p.(Arg69*) variant in *STAG2*; (**D**) Patient 9 with semi-lobar HPE and a c.2683C > G p.(Arg895Gly) variant in *SMC1A*; (**E**) Patient 7 with middle interhemispheric variant HPE and a c.3285+1G > C variant in *SMC1A*; (**F**) Patient 8 with microform HPE and a c.1495C > T p.(Arg499*) variant in *SMC1A*; (**G**) Patient 15 with semi-lobar HPE and an *SMC3* variant c.1138_1152del p.(Gly380_Gln384del). See Table 1 for further details.

Table 3 Phenotype details of individuals with variants in SMC1A

	Present study					Symonds et al., 2017	Jansen et al., 2016	Goldstein et al., 2015	Lebrun et al., 2015	Hoppman-Chaney et al., 2012
	Patient 7	Patient 8	Patient 9	Patient 10	Patient 11	n = 10	n = 2	n = 2	n = 1	n = 1
Variant	c.3285+1G > C	c.1495C > T p.(Arg499*)	c.2683C > G (p. Arg895Gly)	c.2394delA p.(Lys798Asnfs*31)	c.2834delG p.(Gly945Alafs*19)	Truncating variants (n = 10)	Truncating variants (n = 2)	Truncating variants (n = 2)	c.1911+1G > T	8.2-kb deletion in SMC1A; 45,X[7]/ 46,XX[23]
Inheritance	De novo	Singleton	De novo	De novo	De novo	De novo 10/10	De novo 2/2	De novo 2/2	De novo	De novo
Sex	Female	Female	Female	Female	Female	Female 10/10	Female 2/2	Female 2/2	Female	Female
Age	15 months	16.5 months	6 years	3 years	20 months	11 months–14 years	14–46 years	3–4 years	7 years	10 years
Brain MRI	MIHV HPE	Triventricular ectasia	Semi-lobar/lobar HPE	Semi-lobar HPE	Semi-lobar HPE	Semi-lobar HPE 1/10; thin corpus callosum 1/10	Enlarged ventricles and cerebellar vermis hypotrophy (1/2)	Thinning of corpus callosum 1/2	Small frontal lobes, thin corpus callosum	Semi-lobar HPE
Developmental delay	+	+	+	+	+	10/10	2/2	2/2	+	+
Craniofacial anomalies	NR	Single central incisor; depressed nasal bridge	Brachycephaly, synophrys, arched eyebrows, long eyelashes	Synophrys; long eyelashes; upturned nose	Sloping forehead, metopic ridging, upslanting palpebral fissures, midface flattening, bitemporal narrowing	Cleft palate 2/10	Cleft palate 1/2	0/2	Retrognathia	Skull asymmetry with right-sided flattening, Prominent metopic suture, and bitemporal narrowing
Microcephaly	+	+	+	+	+	Average Z-score −3.0 (9/9)	1/2	0/2	+	+
Ear anomalies and hearing	NR	NR	NR	Prominent ears	NR	Posteriorly rotated ears (3/10)	Small ears and prominent anti-helix 1/2	0/2	–	–
Vertebral anomalies	Spina bifida (L-spine)	NR	NR	NR	NR	Bifid thoracic vertebrae 2/10	Scoliosis 2/2	0	–	T7–T12 butterfly vertebrae and partial hemivertebrae
Congenital heart disease	–	–	NR	–	Patent foramen ovale	4/10	0/2	0/2	–	Tetralogy of Fallot
Growth delay	+	+	–	+	NR	Average Z-score −3.0 (9/9)	2/2	1/2	+	+
Limb anomalies	NR	Small hands	Small hands; proximal implant of thumbs	Small hands/feet	NR	Minor limb anomalies 7/10	Small hands 2/2	Small hands/feet 1/2	Small hands/feet	Multiple minor limb anomalies
Other	NR	Seizure disorder; periodic fevers	Seizure disorder; swallowing problems; congenital hip dysplasia; visual impairment	Seizure disorder; feeding problems	Seizure disorder	Seizure disorder 9/9	Seizure disorder 2/2	Seizure disorder 2/2	Seizure disorder; gastro-esophageal reflux	

MIHV = middle interhemispheric variant; NR = not reported.

Table 4 Phenotype details of individuals with LOF variants in RAD21

	Present study			Boyle et al., 2017	Minor et al., 2014		Deardorff et al., 2012b		McBrien et al., 2008	Wuyts et al., 2002
	Patient 12	Patient 13	Patient 14		Patient 1	Patient 2	Patient 1	Patient 4		
Variant	c.1548delinsTC p.Glu518Argfs*19	c.589C>T p.(Gln197*)	c.1217_1224del p.(Lys406Argfs*4)	c.704delG p.(Ser235Ilefs*19)[b]	Heterozygous 665-bp deletion including exon 13	c.592_593dup p.Ser198Argfs*6	Heterozygous chr8:117,708,713– 121,024,193 (hg18) deletion[c]	Heterozygous chr8: 116,950,003– 118,944,486 (hg18) deletion[c]	Heterozygous chr8:117, 640,909– 119,330,085 (hg18) deletion[c]	Heterozygous chr8:117237890– 122631628 (hg18) deletion[c]
Inheritance	Paternal[a]	Unknown	Unknown	Maternal	Maternal	Not found in mother; paternal sample unavailable	De novo	NR	De novo	De novo
Sex	Female	Male	Male	Female	Male	Male	Male	NR	Male	Male
Age	7 years	14 years	2 years	26 years	3 years	12 years	7 years	NR	26 months	18 years
Brain MRI	MIHV	HPE non-specified	Septo-optic dysplasia		Normal	NR	NR	NR	NR	Focal hypersignal in T2 weight images at the level of tuber cinereum
Developmental delay	+	+	+	+	+	+	–	Cognitive delay	Borderline	+
Craniofacial anomalies	Submucous cleft palate; synophrys, hypertelorism	Hypotelorism, up-turned nose, long philtrum	Cleft palate, synophrys, brachycephaly, short nose, long philtrum, thin vermilion border; prominent eyebrows	Long philtrum, thin upper lip vermillion, short nose with up turned nasal tip (from images)	Scaphocephaly, coarse facial features, frontal bossing, mild synophrys, right ptosis, depressed nasal bridge, short nose, micrognathia	Brachycephaly; synophrys; anteverted nose; long philtrum; hirsutism	Full arched eyebrows; synophrys; cleft palate	Thick eyebrows	Prominent metopic ridge; thick eyebrows	Synophrys; long philtrum, and thin vermillion border; hirsutism
Microcephaly	NR	+	+	+	–	+	+	–	+	–
Ear anomalies and hearing	NR	NR	Low-set ears	–	Posteriorly rotated ears	Low-set and posteriorly rotated ears	–	–	NR	–
Vertebral anomalies	NR	NR	–	NR	NR	NR	Thoracic vertebral cleft	NR	Hemivertebrae at T10 and T11	Kyphosis
Congenital heart disease	–	NR	–	–	NR	NR	–	–	Patent foramen ovale	NR
Growth delay	–	–	–	–	+	–	–	+	–	–
Limb anomalies	–	–	Small hands, fifth finger clinodactyly	Fifth finger clinodactyly	Minor hand and feet anomalies	Minor hand and feet anomalies	Minor hand and feet anomalies	Proximal thumb	Minor hand and feet anomalies	Clinodactyly first finger
Other	–	Seizure disorder	Gastroesophageal reflux		Hypospadias; bifid scrotum; undescended testes; inguinal hernia		Exostoses	Exostoses	Bifid scrotum; exostoses	Seizure disorder; exostoses

[a]Father of proband is affected with synophrys, and a submucous cleft palate.

[b]Mother affected with microcephaly and facial features consistent with CdLS.

[c]RAD21 is only cohesin complex gene in minimal overlapping interval (RAD21, EIF3H, UTP23, SLC30A8, MED30, EXT1, RAD21-AS1, AARD).

NR = not reported.

Table 5 Phenotype details of individuals with LOF variants in *SMC3*

	Present study Patient 15	Gil-Rodríguez et al., 2015 n = 16
Variant	c.1138_1152del p.(Gly380_Gln384del)	Missense (9/16); in-frame deletions/duplications (6/16); non-sense (1/16)
Inheritance	*De novo*	*De novo* (10/10)
Sex	Male	Female 7/16
Age	Foetus	NR
Brain imaging	Semilobar HPE	Corpus callosum dysgenesis (2/11); porencephalic cyst (1/11)
Developmental delay	NA	Intellectual disability (13/13)
Craniofacial anomalies	Median cleft lip	Cleft palate 1/14; synophrys (11/15); thick eyebrows (9/13); anteverted nostrils (8/14); thin upper lip vermilion (13/16)
Microcephaly	NR	6/12
Ear anomalies and hearing	NR	Low-set ears (6/11); hearing loss 7/13
Vertebral anomalies	NR	Butterfly vertebrae (1/12); scoliosis (1/12)
Congenital heart disease	Tetralogy of Fallot	9/16
Growth delay	NA	Height Z-score < -3.0 (6/16); weight Z-score < -3.0 (5/16)
Limb anomalies	Hand/feet cutaneous syndactyly; ulnar deviation of second digit of hands bilaterally; proximally set thumbs	Small hands (11/14); small feet (11/13); proximally set thumbs (12/16)
Other	Hypospadias; anal atresia	Seizures (3/12)

NA = non-applicable; NR = not reported.

12–14) (Ansari *et al.*, 2014; Boyle *et al.*, 2015; Yuan *et al.*, 2015) and are most commonly missense and in-frame deletions (Huisman *et al.*, 2013). Four of five individuals in the present study had LOF variants; therefore, we used 16 cases with LOF variants in *SMC1A* from the medical literature with phenotype information for comparison in Table 3 (Hoppman-Chaney *et al.*, 2012; Goldstein *et al.*, 2015; Lebrun *et al.*, 2015; Jansen *et al.*, 2016; Symonds *et al.*, 2017). The most severe phenotype in the LOF variants in the medical literature was HPE found in 2 of 16 individuals (Hoppman-Chaney *et al.*, 2012; Symonds *et al.*, 2017). In both the present study and in the medical literature, when parents were available, all LOF variants were *de novo* and all individuals were females. In addition to midline brain defects, the most striking phenotype is seizure disorders. In the present study, four of five individuals had seizures and 15 of 16 in the medical literature. In the largest study of 10 individuals with truncating variants in *SMC1A*, nine of nine reporting seizures had severe drug-resistant epilepsy (Symonds *et al.*, 2017). All 16 cases in the present study and medical literature had developmental delay. Two individuals in the present study have facial characteristics consistent with mild CdLS, Patients 9 and 10 both had synophrys and small hands. In the largest study of LOF variants in *SMC1A* (Table 3), the authors report few phenotype characteristics consistent with CdLS (Symonds *et al.*, 2017).

RAD21

Four variants were found in the two cohesin complex genes that are not X-linked, three were in the gene *RAD21*. The three *RAD21* variants (Patients 12 and 13) (Table 4) were LOF; interestingly, Patient 12 with the c.1548delinsTC

p.(Glu518Argfs*19) variant in *RAD21* is a paternally inherited variant with the father having synophrys and a submucous cleft palate. In Table 4, the three LOF variants in the present study are compared to LOF and deletions involving *RAD21* in the medical literature (Wuyts *et al.*, 2002; McBrien *et al.*, 2008; Deardorff *et al.*, 2012b; Minor *et al.*, 2014; Boyle *et al.*, 2017). A much higher fraction of LOF variants are inherited compared to *STAG2* and *SMC1A*: present study one (1/1) and in the medical literature, 2 of 5 (when parents where available). Both the present study and the medical literature presented individuals with cardinal features of CdLS (Kline *et al.*, 2018), including: synophrys or thick eyebrows in 8/10, short or upturned nose in 5/10, long philtrum 5/10, and microcephaly in 6/10.

SMC3

The fourth non-X-linked gene is *SMC3* and the *SMC3* variant (Patient 15; Table 5) was a *de novo* in-frame deletion that is likely pathogenic (Richards *et al.*, 2015). In Table 5, we compare to the largest and most comprehensive series of individuals with variants in *SMC3* (n = 16) (Gil-Rodríguez *et al.*, 2015). The present study found an in-frame deletion in *SMC3* in a foetus with semilobar HPE, median cleft lip, tetralogy of Fallot, hypospadias, anal atresia and limb anomalies. Gil-Rodríguez *et al.* (2015) found two of their study participants to have midline brain malformations: corpus callosum dysgenesis (2/11) and no cases of holoprosencephaly. Based on reviewing the present study's case and the cohort presented by Gil-Rodríguez *et al.*, intellectual disability (13/13) and congenital heart disease (10/17) were prevalent. The facial features are difficult to characterize because of the early gestation in the present study
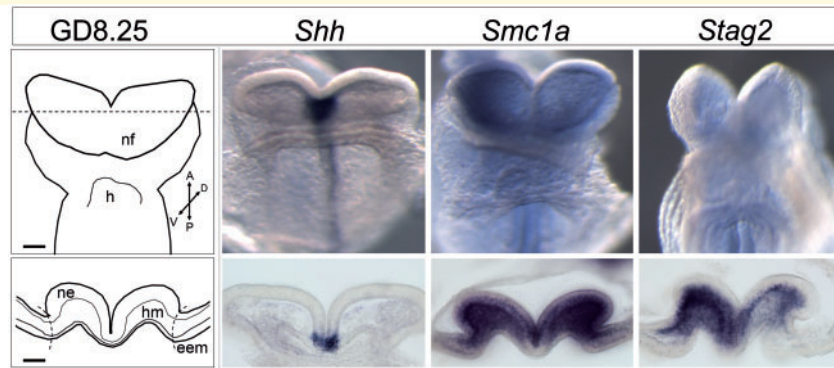
Figure 2 Gestational day (GD) 8.25 mouse embryos were stained by *in situ* hybridization to determine gene expression patterns. A ventral view is shown for whole mounts. Transverse sections through the prosencephalic neural folds (at the level of the dashed line in schematic) were stained to visualize gene expression in specific cellular compartments. eem = extra-embryonic membranes; h = heart; hm = head mesenchyme; ne = neuroectoderm; nf = neural folds. Scale bar = 100 μm.

(Fig. 1G); however, Gil-Rodríguez *et al.* found a majority of cases to have facial features consistent with CdLS (Table 5).

Mouse *in situ* hybridization

As a control, we first examined the expression of *Shh* (Fig. 2), a gene with a well-characterized expression domain and role in forebrain patterning and HPE (Chiang *et al.*, 1996; Solomon *et al.*, 2012; Hong *et al.*, 2016). Expression of *Shh* is restricted to the ventromedial neuro-ectoderm (Fig. 2) as described previously (Echelard *et al.*, 1993). Both *Smc1a* and *Stag2* are also strongly detected in the anterior neural folds with expression observed in both the neuro-ectoderm and adjacent mesenchyme (Fig. 2). The specificity of the observed expression domains for these genes is supported by the absence of staining in extra-embryonic membrane tissue lateral to the neural folds.

Gene expression studies in human neural stem cells

As noted in the 'Materials and methods' section, we analysed the expression level of genes known to be involved in HPE pathways with RT-qPCR, which include *SHH*, *SIX3*, *FGFR1*, *GLI2*, *ZIC2*, *GLI2*, *SMAD3* and *DISP1*. *SHH*, *SIX3*, *ZIC2* and *FGFR1* were chosen as variants in these genes known to cause HPE (Kruszka *et al.*, 2018; Kruszka and Muenke, 2018). *DISP1* is part of the sonic hedgehog pathway and has been associated with HPE (Roessler *et al.*, 2009; Dubourg *et al.*, 2016); also part of the sonic hedgehog pathway, *GLI2* is an often HPE tested gene that is associated with HPE spectrum anomalies including pituitary insufficiency, midface hypoplasia, hypotelorism, and cleft lip/palate (Kruszka *et al.*, 2018). Although not known to contain driver mutations associated with HPE, SMAD3 physically interacts with ZIC2 and controls

transcription in a NODAL-dependent manner and variant forms of ZIC2 associated with HPE in humans and the mouse have difficulty with SMAD-dependent transcription, making *SMAD3* of interest (Houtmeyers *et al.*, 2016). Compared to controls, *SMC1A* knockdown in human neural stems cells resulted in significantly increased expression in *GLI2* ($P < 0.01$), ZIC2 ($P < 0.05$), and SMAD3 ($P < 0.05$) (Supplementary Fig. 2). For *STAG2* knockdown (Supplementary Fig. 3), significantly increased expression was seen in ZIC2 ($P < 0.0001$) and *FGFR1* ($P < 0.01$). Thus, there was overexpression in *ZIC2* from knockdown of both *SMC1A* and *STAG2*. Similar to a previous experiment (Cotney *et al.*, 2015), *SHH* and *SIX3* expression was undetectable in human neural stem cells.

Discussion

HPE research and clinical care has focused on sonic hedgehog pathway and the genes *SHH*, *ZIC2*, and *SIX3* for the last two decades (Roessler and Muenke, 2010; Roessler *et al.*, 2018). This study introduces new genes in the cohesin complex as important components of early forebrain division and the holoprosencephaly spectrum. Evaluating the holoprosencephaly study at NHGRI with WES, five of 277 probands were identified with variants in cohesin complex genes. Ten additional individuals with HPE were identified from other institutions. Eleven of the 15 individuals had variants in the X-linked genes *STAG2* and *SMC1A*. *STAG2* has only recently been associated with human disease (Mullegama *et al.*, 2017, 2019; Soardi *et al.*, 2017; Aoi *et al.*, 2019; Yuan *et al.*, 2019). A small number of cases with cohesin complex HPE have been reported in the medical literature in the past: two HPE cases with LOF variants in *STAG2* (Aoi *et al.*, 2019; Yuan *et al.*, 2019), two cases associated with *SMC1A* (Hoppman-Chaney *et al.*, 2012; Symonds *et al.*, 2017), and no HPE cases have been reported that we are aware of in *RAD21*

and *SMC3*. Knowing that all individuals with CdLS have not had brain imaging, the incidence of HPE associated with cohesinopathy genes may be more common than previously reported.

Interestingly, the 11 individuals in this study with *STAG2* and *SMC1A* variants were females, thus we propose that LOF variants in the X-linked cohesin genes are usually lethal in males; certainly, there are possible exceptions in males including mosaicism, 47,XXY, and gene duplications. Notably, *STAG2* undergoes complete X-inactivation and *SMC1A* undergoes partial X-inactivation (Cotton *et al.*, 2013). For Patient 2 with a *STAG2* nonsense variant (c.205C>T p.(Arg69*)), X-inactivation studies were consistent with random X-inactivation, implying that haploinsufficiency is required for the HPE phenotype in *STAG2*. The one exception to LOF in *STAG2* and *SMC1A* is Patient 9, who had a missense variant (Table 1) located in the conserved second coiled-coil domain and is likely pathogenic (Richards *et al.*, 2015). Based on the LOF variants in *SMC1A* in the other four individuals in this report, we hypothesize that the *SMC1A* variant (c.2683C>G (p. Arg895Gly)) has a LOF variant or a dominant negative effect. To evaluate X-linked inheritance from our HPE registry, we performed a binomial distribution on 700 individuals with HPE. Of these 700 individuals, 409 were female ($P = 0.000005$). If we subtract individuals with known pathogenic variants in *SHH*, *SIX*, and *ZIC2*, there are 645 individuals, of whom, 378 were female ($P = 0.000015$). Although *STAG2* and *SMC1A* variation most likely does not explain this significant trend towards female sex in our registry, X-linked dominant inheritance likely plays an important role.

A previous study has shown that antagonizing the hedgehog signalling pathway between gestational days 7.0 and 8.25 of mouse development (approximately corresponding to the 15th to 22nd days of human gestation) results in HPE (Heyne *et al.*, 2015a). As forebrain patterning genes are expected to be expressed in the prosencephalic neural folds during primary neurulation (Geng and Oliver, 2009), we assessed expression of cohesin complex genes during this critical period for HPE in the mouse. The finding that both *Smc1a* and *Stag2* are expressed in the prosencephalic neural folds complements the human genetic evidence in this study and supports the role of cohesion complex genes in forebrain morphogenesis. Being expressed in both the neuro-ectoderm and adjacent mesenchyme suggests that the cohesion complex may interact with other critical regulators of forebrain patterning and HPE pathogenesis.

To elucidate the relationship between forebrain division in early embryogenesis and the cohesin complex further, we knocked down cohesin complex gene expression in human progenitor cells and measured canonical HPE gene expression. Upregulation in gene expression was seen in *GLI2*, *ZIC2* and *SMAD3* for *SMC1A* knockdown (Supplementary Fig. 2), and *ZIC2* and *FGFR1* for *STAG2* knockdown (Supplementary Fig. 3). LOF in *ZIC2* has been associated with HPE in the past and the mechanism of increased *ZIC2* expression in *SMC1A* and *STAG2* knockdown human neural stem cells is not completely clear. In the mouse model, LOF of *Zic2* results in the failure to activate specific genes in the mid-gastrula node including *Foxa2*, which is required to activate *Shh* in the prechordal plate (Warr *et al.*, 2008). There is evidence in the *Xenopus* that overexpression of *zic2* may contribute depletion of *foxa2* in the Spemann organizer (Houtmeyers *et al.*, 2016). Overexpression by injection of *zic2* mRNA into *Xenopus* embryos at the four- to eight-cell stage resulted in reduced *foxa2* expression (Houtmeyers *et al.*, 2016). *SMAD3* is upregulated in *SMC1A* knockdown, which is of interest as SMAD3 and ZIC2 physically interact with each other in cell culture (A549 cells) to occupy a binding site in the promoter region of *FOXA2* (Houtmeyers *et al.*, 2016). *FGFR1* expression increased in *STAG2* knockdown neural progenitor cells. *FGFR1* variants are associated with Hartsfield syndrome, which has HPE and split hands and feet as phenotype elements. It is unclear how overexpression of *FGFR1* is related to HPE as the mechanism of *FGFR1* in HPE is a dominant negative effect (Hong *et al.*, 2016). *GLI2* is overexpressed in the *SMC1A* knockdown neural progenitor cells. GLI2 is both a transcriptional activator and repressor in the sonic hedgehog pathway (Sasaki *et al.*, 1999) and although it does not cause HPE, LOF variants in *GLI2* are associated with Culler-Jones syndrome, which presents with hypopituitarism, polydactyly and facial features often found in HPE (Kruszka *et al.*, 2018).

In conclusion, we present 15 patients with HPE spectrum malformations who have variants in cohesin complex genes *STAG2*, *SMC1A*, *SMC3* and *RAD21*. Although the precise mechanism of abnormal forebrain development is unknown in LOF variants in cohesin complex genes, *Stag2* and *Smc1a* are expressed in neural fold at the critical time of forebrain division in the mouse model. Additionally, we show that knockdown of *STAG2* and *SMC1A* in human neural stem cells perturbs known HPE genes. Currently, there are no cohesin complex or X-linked genes that are commonly tested for in individuals with HPE (Kruszka *et al.*, 2018). This report of X-linked and cohesin complex HPE has broad implications for future genetic testing, genetic counselling and HPE research.

Acknowledgements

Funding

Competing interests

The authors report no competing interests.

Supplementary material

Supplementary material is available at *Brain* online.

References

Ansari M, Poke G, Ferry Q, Williamson K, Aldridge R, Meynert AM, et al. Genetic heterogeneity in Cornelia de Lange syndrome (CdLS) and CdLS-like phenotypes with observed and predicted levels of mosaicism. J Med Genet 2014; 51: 659–68.

Aoi H, Lei M, Mizuguchi T, Nishioka N, Goto T, Miyama S, et al. Nonsense variants in STAG2 result in distinct sex-dependent phenotypes. J Hum Genet 2019; 64: 487–92.

Boyle MI, Jespersgaard C, Brondum-Nielsen K, Bisgaard AM, Tumer Z. Cornelia de Lange syndrome. Clin Genet 2015; 88: 1–12.

Boyle MI, Jespersgaard C, Nazaryan L, Bisgaard AM, Tumer Z. A novel RAD21 variant associated with intrafamilial phenotypic variation in Cornelia de Lange syndrome: review of the literature. Clin Genet 2017; 91: 647–9.

Brooker AS, Berkowitz KM. The roles of cohesins in mitosis, meiosis, and human health and disease. Methods Mol Biol 2014; 1170: 229–66.

Chetaille P, Preuss C, Burkhard S, Cote JM, Houde C, Castilloux J, et al. Mutations in SGOL1 cause a novel cohesinopathy affecting heart and gut rhythm. Nat Genet 2014; 46: 1245–9.

Chiang C, Litingtung Y, Lee E, Young KE, Corden JL, Westphal H, et al. Cyclopia and defective axial patterning in mice lacking Sonic hedgehog gene function. Nature 1996; 383: 407–13.

Cotney J, Muhle RA, Sanders SJ, Liu L, Willsey AJ, Niu W, et al. The autism-associated chromatin modifier CHD8 regulates other autism risk genes during human neurodevelopment. Nat Commun 2015; 6: 6404.

Cotton AM, Ge B, Light N, Adoue V, Pastinen T, Brown CJ. Analysis of expressed SNPs identifies variable extents of expression from the human inactive X chromosome. Genome Biol 2013; 14: R122.

De Franco E, Watson RA, Weninger WJ, Wong CC, Flanagan SE, Caswell R, et al. A Specific CNOT1 mutation results in a novel syndrome of pancreatic agenesis and holoprosencephaly through impaired pancreatic and neurological development. Am J Hum Genet 2019; 104: 985–9.

Deardorff MA, Bando M, Nakato R, Watrin E, Itoh T, Minamino M, et al. HDAC8 mutations in Cornelia de Lange syndrome affect the cohesin acetylation cycle. Nature 2012a; 489: 313–7.

Deardorff MA, Kaur M, Yaeger D, Rampuria A, Korolev S, Pie J, et al. Mutations in cohesin complex members SMC3 and SMC1A cause a mild variant of cornelia de Lange syndrome with predominant mental retardation. Am J Hum Genet 2007; 80: 485–94.

Deardorff MA, Wilde JJ, Albrecht M, Dickinson E, Tennstedt S, Braunholz D, et al. RAD21 mutations cause a human cohesinopathy. Am J Hum Genet 2012b; 90: 1014–27.

Dubourg C, Carre W, Hamdi-Roze H, Mouden C, Roume J, Abdelmajid B, et al. Mutational spectrum in holoprosencephaly shows that FGF is a new major signaling pathway. Hum Mutat 2016; 37: 1329–39.

Echelard Y, Epstein DJ, St-Jacques B, Shen L, Mohler J, McMahon JA, et al. Sonic hedgehog, a member of a family of putative signaling molecules, is implicated in the regulation of CNS polarity. Cell 1993; 75: 1417–30.

Everson JL, Fink DM, Yoon JW, Leslie EJ, Kietzman HW, Ansen-Wilson LJ, et al. Sonic Hedgehog regulation of Foxf2 promotes cranial neural crest mesenchyme proliferation and is disrupted in cleft lip morphogenesis. Development 2017; 144: 2082–91.

Firth HV, Richards SM, Bevan AP, Clayton S, Corpas M, Rajan D, et al. DECIPHER: database of chromosomal imbalance and phenotype in humans using ensembl resources. Am J Hum Genet 2009; 84: 524–33.

Geng X, Oliver G. Pathogenesis of holoprosencephaly. J Clin Invest 2009; 119: 1403–13.

Gil-Rodríguez MC, Deardorff MA, Ansari M, Tan CA, Parenti I, Baquero-Montoya C, et al. De novo heterozygous mutations in SMC3 cause a range of Cornelia de Lange syndrome-overlapping phenotypes. Hum Mutat 2015; 36: 454–62.

Goldstein JH, Tim-Aroon T, Shieh J, Merrill M, Deeb KK, Zhang S, et al. Novel SMC1A frameshift mutations in children with developmental delay and epilepsy. Eur J Med Genet 2015; 58: 562–8.

Gordillo M, Vega H, Trainer AH, Hou F, Sakai N, Luque R, et al. The molecular mechanism underlying Roberts syndrome involves loss of ESCO2 acetyltransferase activity. Hum Mol Genet 2008; 17: 2172–80.

Hahn JS, Barnes PD, Clegg NJ, Stashinko EE. Septopreoptic holoprosencephaly: a mild subtype associated with midline craniofacial anomalies. AJNR Am J Neuroradiol 2010; 31: 1596–601.

Heyne GW, Melberg CG, Doroodchi P, Parins KF, Kietzman HW, Everson JL, et al. Definition of critical periods for Hedgehog pathway antagonist-induced holoprosencephaly, cleft lip, and cleft palate. PLoS One 2015a; 10: e0120517.

Heyne GW, Plisch EH, Melberg CG, Sandgren EP, Peter JA, Lipinski RJ. A simple and reliable method for early pregnancy detection in inbred mice. J Am Assoc Lab Anim Sci 2015b; 54: 368–71.

Hong S, Hu P, Marino J, Hufnagel SB, Hopkin RJ, Toromanovic A, et al. Dominant-negative kinase domain mutations in FGFR1 can explain the clinical severity of Hartsfield syndrome. Hum Mol Genet 2016; 25: 1912–22.

Hoppman-Chaney N, Jang JS, Jen J, Babovic-Vuksanovic D, Hodge JC. In-frame multi-exon deletion of SMC1A in a severely affected female with Cornelia de Lange Syndrome. Am J Med Genet A 2012; 158A: 193–8.

Houtmeyers R, Tchouate Gainkam O, Glanville-Jones HA, Van den Bosch B, Chappell A, Barratt KS, et al. Zic2 mutation causes holoprosencephaly via disruption of NODAL signalling. Hum Mol Genet 2016; 25: 3946–59.

Huisman SA, Redeker EJ, Maas SM, Mannens MM, Hennekam RC. High rate of mosaicism in individuals with Cornelia de Lange syndrome. Journal of medical genetics 2013; 50: 339–44.

Izumi K, Nakato R, Zhang Z, Edmondson AC, Noon S, Dulik MC, et al. Germline gain-of-function mutations in AFF4 cause a developmental syndrome functionally linking the super elongation complex and cohesin. Nat Genet 2015; 47: 338–44.

Jansen S, Kleefstra T, Willemsen MH, de Vries P, Pfundt R, Hehir-Kwa JY, et al. De novo loss-of-function mutations in X-linked SMC1A cause severe ID and therapy-resistant epilepsy in females: expanding the phenotypic spectrum. Clin Genet 2016; 90: 413–9.

Kircher M, Witten DM, Jain P, O'Roak BJ, Cooper GM, Shendure J. A general framework for estimating the relative pathogenicity of human genetic variants. Nat Genet 2014; 46: 310–5.

Kline AD, Moss JF, Selicorni A, Bisgaard AM, Deardorff MA, Gillett PM, et al. Diagnosis and management of Cornelia de Lange syndrome: first international consensus statement. Nat Rev Genet 2018; 19: 649–66.

Krantz ID, McCallum J, DeScipio C, Kaur M, Gillis LA, Yaeger D, et al. Cornelia de Lange syndrome is caused by mutations in NIPBL, the human homolog of Drosophila melanogaster Nipped-B. Nat Genet 2004; 36: 631–5.

Kruszka P, Berger SI, Weiss K, Everson JL, Martinez AF, Hong S, et al. CCR4-NOT transcription complex, subunit 1 (CNOT1) variant associated with holoprosencephaly. Am J Hum Genet 2019; 104: 990–3.

Kruszka P, Martinez AF, Muenke M. Molecular testing in holoprosencephaly. Am J Med Genet C 2018; 178: 187–93.

Kruszka P, Muenke M. Syndromes associated with holoprosencephaly. Am J Med Genet C 2018; 178: 229–37.

Lebrun N, Lebon S, Jeannet PY, Jacquemont S, Billuart P, Bienvenu T. Early-onset encephalopathy with epilepsy associated with a novel splice site mutation in SMC1A. Am J Med Genet A 2015; 167A: 3076–81.

Lek M, Karczewski KJ, Minikel EV, Samocha KE, Banks E, Fennell T, et al. Analysis of protein-coding genetic variation in 60,706 humans. Nature 2016; 536: 285–91.

Matsunaga E, Shiota K. Holoprosencephaly in human embryos: epidemiologic studies of 150 cases. Teratology 1977; 16: 261–72.

McBrien J, Crolla JA, Huang S, Kelleher J, Gleeson J, Lynch SA. Further case of microdeletion of 8q24 with phenotype overlapping Langer-Giedion without TRPS1 deletion. Am J Med Genet A 2008; 146A: 1587–92.

Mehta GD, Kumar R, Srivastava S, Ghosh SK. Cohesin: functions beyond sister chromatid cohesion. FEBS Lett 2013; 587: 2299–312.

Minor A, Shinawi M, Hogue JS, Vineyard M, Hamlin DR, Tan C, et al. Two novel RAD21 mutations in patients with mild Cornelia de Lange syndrome-like presentation and report of the first familial case. Gene 2014; 537: 279–84.

Mullegama SV, Klein SD, Mulatinho MV, Senaratne TN, Singh K, Center UCG, et al. De novo loss-of-function variants in STAG2 are associated with developmental delay, microcephaly, and congenital anomalies. Am J Med Genet A 2017; 173: 1319–27.

Mullegama SV, Klein SD, Signer RH, Center UCG, Vilain E, Martinez-Agosto JA. Mutations in STAG2 cause an X-linked cohesinopathy associated with undergrowth, developmental delay, and dysmorphia: expanding the phenotype in males. Mol Genet Genomic Med 2019; 7: e00501.

Musio A, Selicorni A, Focarelli ML, Gervasini C, Milani D, Russo S, et al. X-linked Cornelia de Lange syndrome owing to SMC1L1 mutations. Nat Genet 2006; 38: 528–30.

Olley G, Ansari M, Bengani H, Grimes GR, Rhodes J, von Kriegsheim A, et al. BRD4 interacts with NIPBL and BRD4 is mutated in a Cornelia de Lange-like syndrome. Nat Genet 2018; 50: 329–32.

Pineda-Alvarez DE, Dubourg C, David V, Roessler E, Muenke M. Current recommendations for the molecular evaluation of newly diagnosed holoprosencephaly patients. Am J Med Genet C 2010; 154C: 93–101.

Richards S, Aziz N, Bale S, Bick D, Das S, Gastier-Foster J, et al. Standards and guidelines for the interpretation of sequence variants: a joint consensus recommendation of the American College of Medical Genetics and Genomics and the Association for Molecular Pathology. Genet Med 2015; 17: 405–24.

Roessler E, Hu P, Muenke M. Holoprosencephaly in the genomics era. Am J Med Genet C 2018; 178: 165–74.

Roessler E, Ma Y, Ouspenskaia MV, Lacbawan F, Bendavid C, Dubourg C, et al. Truncating loss-of-function mutations of DISP1 contribute to holoprosencephaly-like microform features in humans. Hum Genet 2009; 125: 393–400.

Roessler E, Muenke M. The molecular genetics of holoprosencephaly. Am J Med Genet C 2010; 154C: 52–61.

Sasaki H, Nishizaki Y, Hui C, Nakafuku M, Kondoh H. Regulation of Gli2 and Gli3 activities by an amino-terminal repression domain: implication of Gli2 and Gli3 as primary mediators of Shh signaling. Development 1999; 126: 3915–24.

Simonis N, Migeotte I, Lambert N, Perazzolo C, de Silva DC, Dimitrov B, et al. FGFR1 mutations cause Hartsfield syndrome, the unique association of holoprosencephaly and ectrodactyly. J Med Genet 2013; 50: 585–92.

Soardi FC, Machado-Silva A, Linhares ND, Zheng G, Qu Q, Pena HB, et al. Familial STAG2 germline mutation defines a new human cohesinopathy. NPJ Genom Med 2017; 2: 7.

Sobreira N, Schiettecatte F, Valle D, Hamosh A. GeneMatcher: a matching tool for connecting investigators with an interest in the same gene. Hum Mutat 2015; 36: 928–30.

Solomon BD, Bear KA, Wyllie A, Keaton AA, Dubourg C, David V, et al. Genotypic and phenotypic analysis of 396 individuals with mutations in Sonic Hedgehog. J Med Genet 2012; 49: 473–9.

Symonds JD, Joss S, Metcalfe KA, Somarathi S, Cruden J, Devlin AM, et al. Heterozygous truncation mutations of the SMC1A gene cause a severe early onset epilepsy with cluster seizures in females: detailed phenotyping of 10 new cases. Epilepsia 2017; 58: 565–75.

Warr N, Powles-Glover N, Chappell A, Robson J, Norris D, Arkell RM. Zic2-associated holoprosencephaly is caused by a transient defect in the organizer region during gastrulation. Hum Mol Genet 2008; 17: 2986–96.

Wuyts W, Roland D, Ludecke HJ, Wauters J, Foulon M, Van Hul W, et al. Multiple exostoses, mental retardation, hypertrichosis, and brain abnormalities in a boy with a de novo 8q24 submicroscopic interstitial deletion. Am J Med Genet 2002; 113: 326–32.

Yuan B, Neira J, Pehlivan D, Santiago-Sim T, Song X, Rosenfeld J, et al. Clinical exome sequencing reveals locus heterogeneity and phenotypic variability of cohesinopathies. Genet Med 2019; 21: 663–75.

Yuan B, Pehlivan D, Karaca E, Patel N, Charng WL, Gambin T, et al. Global transcriptional disturbances underlie Cornelia de Lange syndrome and related phenotypes. J Clin Invest 2015; 125: 636–51.